Supporting Information

Designing type V deep eutectic solvents with antimalarial pharmaceutical ingredients

Gabriel Teixeira[†], Paula Brandão[†], Ana I. M. C. Lobo Ferreira[ǂ], Dinis O. Abranches[†], Luís M. N. B. F. Santos[ǂ], Olga Ferreira[‡,§,*], João A. P. Coutinho[†]

[†]CICECO, Aveiro Institute of Materials, Complexo de Laboratórios Tecnológicos, University of Aveiro, Campus Universitário de Santiago, Aveiro, Portugal

[ǂ]CIQUP, Institute of Molecular Sciences (IMS), Departamento de Química e Bioquímica, Faculdade de Ciências da Universidade do Porto, Rua Campo Alegre, 4169-007 Porto, Portugal

[‡]Centro de Investigação de Montanha (CIMO), Instituto Politécnico de Bragança, Campus de Santa Apolónia, 5300-253 Bragança, Portugal

[§]Laboratório para a Sustentabilidade e Tecnologia em Regiões de Montanha, Instituto Politécnico de Bragança, Campus de Santa Apolónia, 5300-253 Bragança, Portugal

*Corresponding author: Olga Ferreira, E-mail address: oferreira@ipb.pt, Phone: +351 273 303 087

Estimated and calculated uncertainties, and statistical analysis

The uncertainty of the experimental results of single measurements obtained by Visual Method is estimated to be 2.0 K, and by DSC is estimated to be 1.0 K. The uncertainties of the results of multiple repetitions are obtained from the standard deviation ($s = \sqrt{\frac{\sum(T_i - \overline{T})^2}{n-1}}$, where T is the transition temperature, $\overline{T}$ is the mean of the transition temperatures and n is the number of repetitions).

The calculated uncertainties of mole fraction and activity coefficients are obtained through error propagation theory considering the analytical balance accuracy (± 0.002 g), melting temperature uncertainties mentioned above, and uncertainty of melting properties of the pure compounds (See Table 1).

Figures

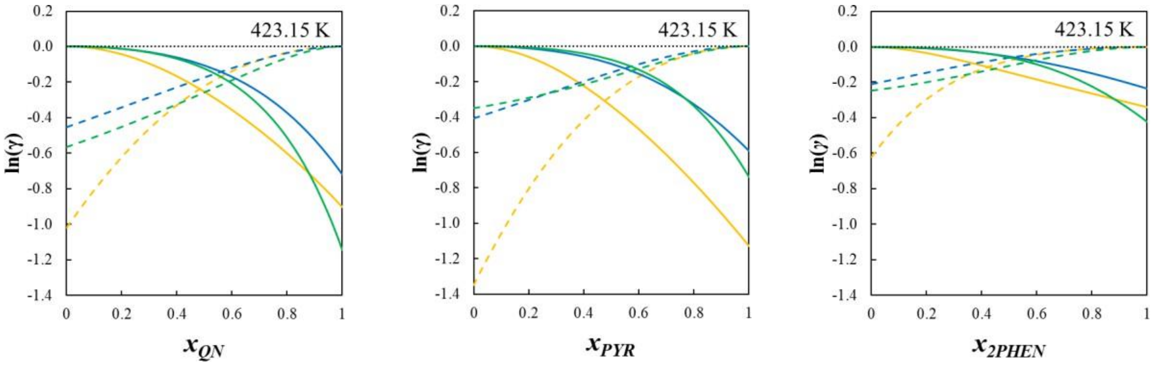

Figure S.1 – Activity coefficients predictions of COSMO-RS (TZVP) at 423.15 K of mixtures of QN (left), PYR (center) and 2PHEN (right) with THY (green), PG (yellow) and BHA (blue). The activity coefficients of QN, PYR and 2PHEN are represented by dashed lines, and of THY, PG and BHA by solid lines. Dotted horizontal lines represent the ideal behaviour, $\ln(\gamma_i) = 0$.

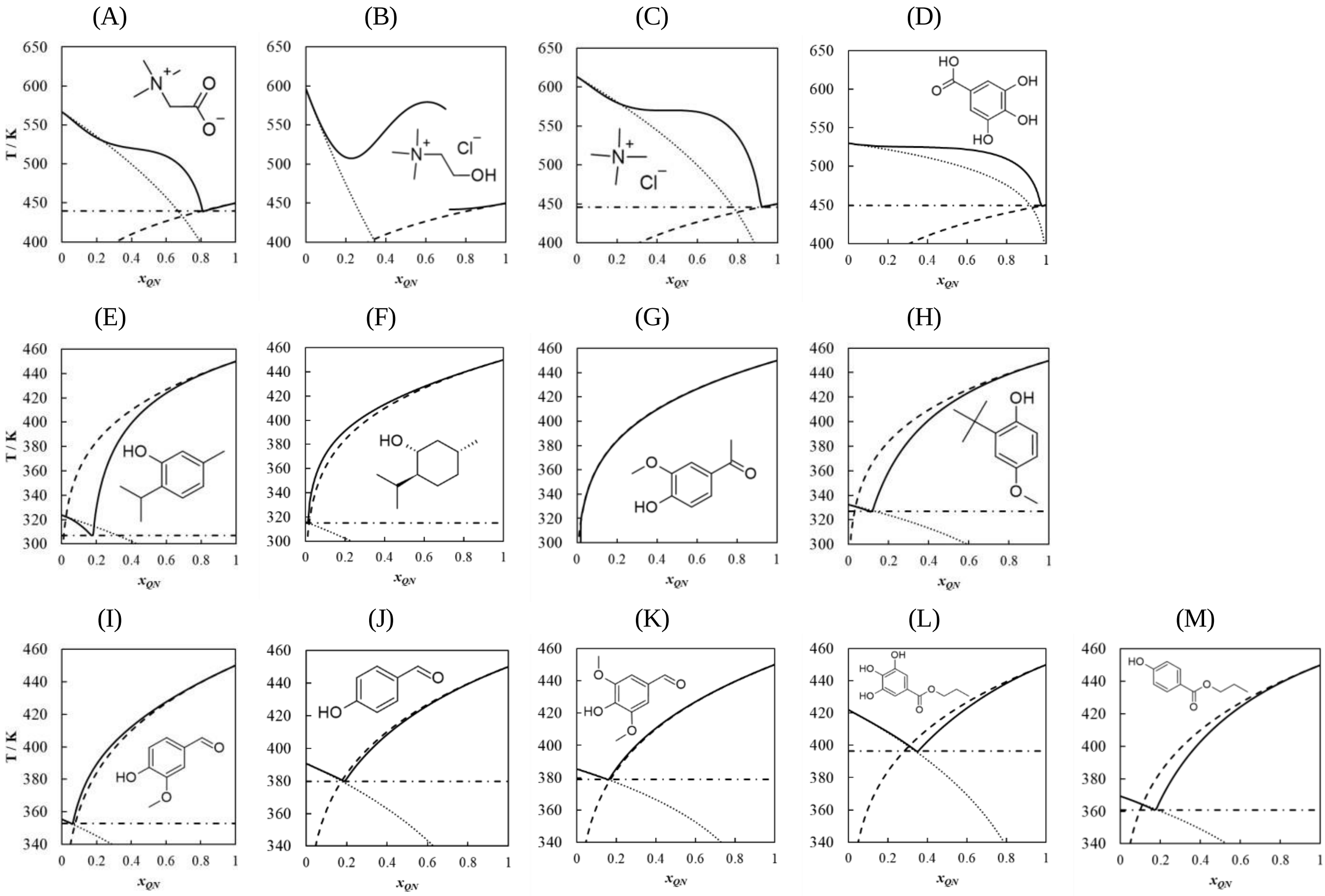

Figure S.2 – Solid-liquid phase diagrams of quinine with (A) betaine, (B) choline chloride, (C) $[N_{1111}][Cl]$, (D) gallic acid, (E) thymol, (F) (-)-menthol, (G) acetovanillone, (H) 3-butylated hydroxyanisole, (I) vanillin, (J) 4-hydroxybenzaldehyde, (K) syringaldehyde, (L) propyl gallate and (M) propylparaben. Lines represent the ideal model of quinine (dashed line), ideal model of the excipient (dotted line), COSMO-RS TZVP model predictions of the liquidus temperature (solid line) and the predicted eutectic temperature (dash-dotted line). Melting properties used are presented in Table 1 and Table S.13.

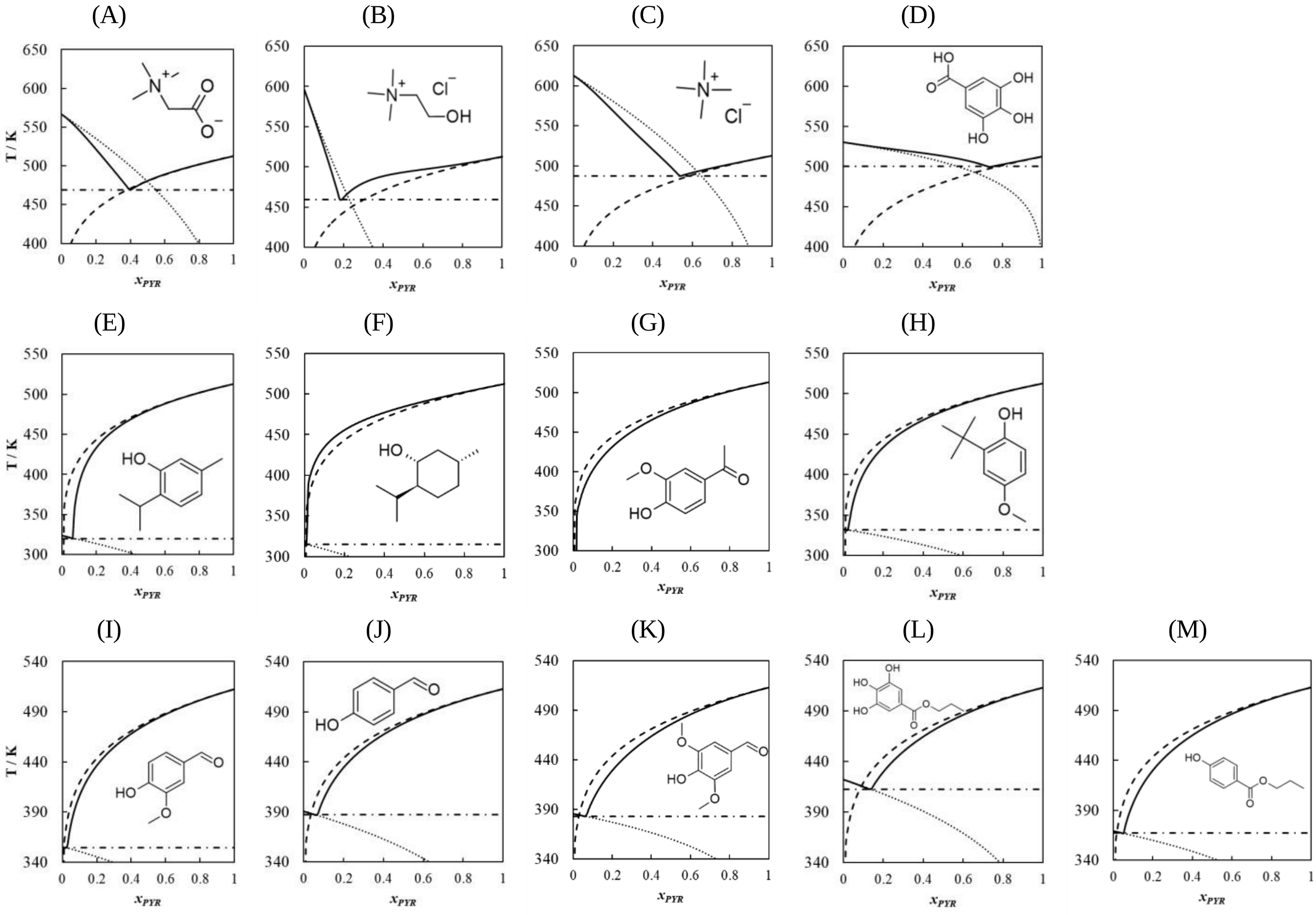

Figure S.3 – Solid-liquid phase diagrams of pyrimethamine with (A) betaine, (B) choline chloride, (C) [N_{1111}][Cl], (D) gallic acid, (E) thymol, (F) (-)-menthol, (G) acetovanillone, (H) 3-butylated hydroxyanisole, (I) vanillin, (J) 4-hydroxybenzaldehyde, (K) syringaldehyde, (L) propyl gallate and (M) propylparaben. Lines represent the ideal model of pyrimethamine (dashed line), ideal model of the excipient (dotted line), COSMO-RS TZVP model predictions of the liquidus temperature (solid line) and the predicted eutectic temperature (dash-dotted line). Melting properties used are presented in Table 1 and Table S.13.

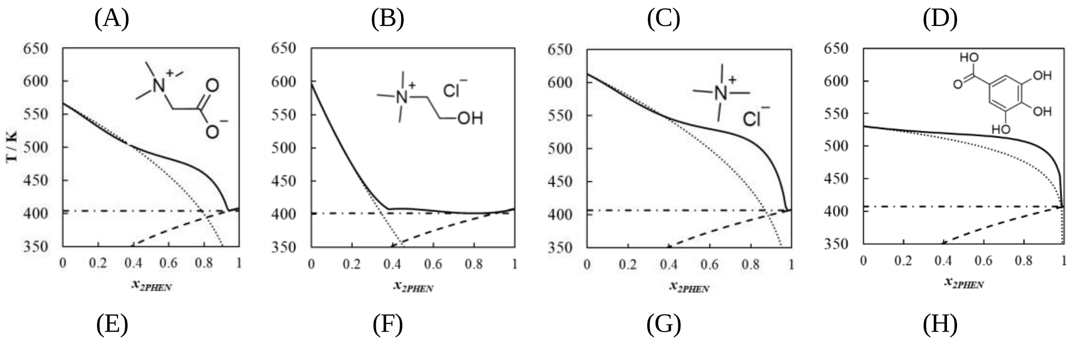

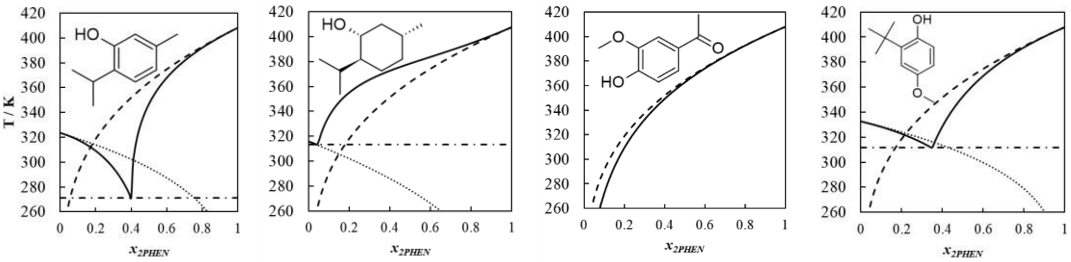

(I) (J) (K) (L) (M)

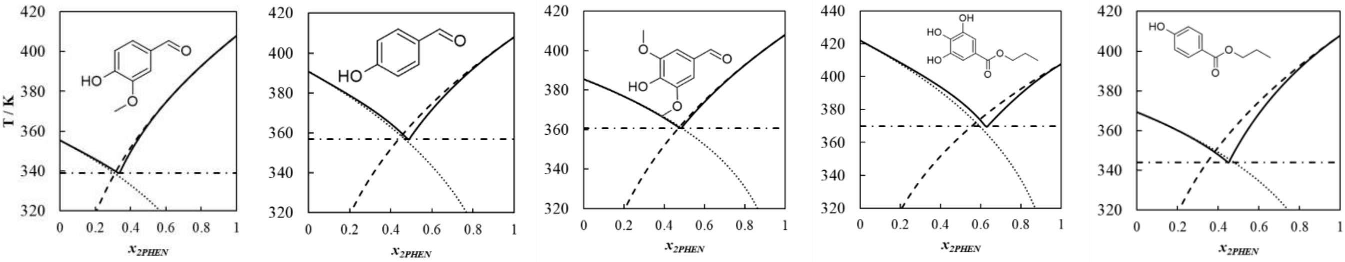

Figure S.4 – Solid-liquid phase diagrams of 2-phenylimidazopyridine with (A) betaine, (B) choline chloride, (C) $[N_{1111}][Cl]$, (D) gallic acid, (E) thymol, (F) (-)-menthol, (G) acetovanillone, (H) 3-butylated hydroxyanisole, (I) vanillin, (J) 4-hydroxybenzaldehyde, (K) syringaldehyde, (L) propyl gallate and (M) propylparaben. Lines represent the ideal model of 2-phenylimidazopyridine (dashed line), ideal model of the excipient (dotted line), COSMO-RS TZVP model predictions of the liquidus temperature (solid line) and the predicted eutectic temperature (dash-dotted line). Melting properties used are presented in Table 1 and Table S.13.

(A) (B) (C)

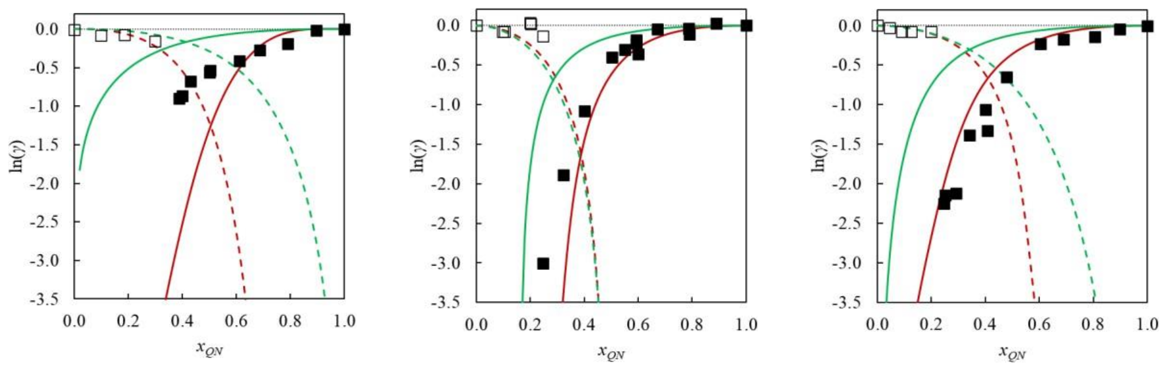

(D) (E) (F)

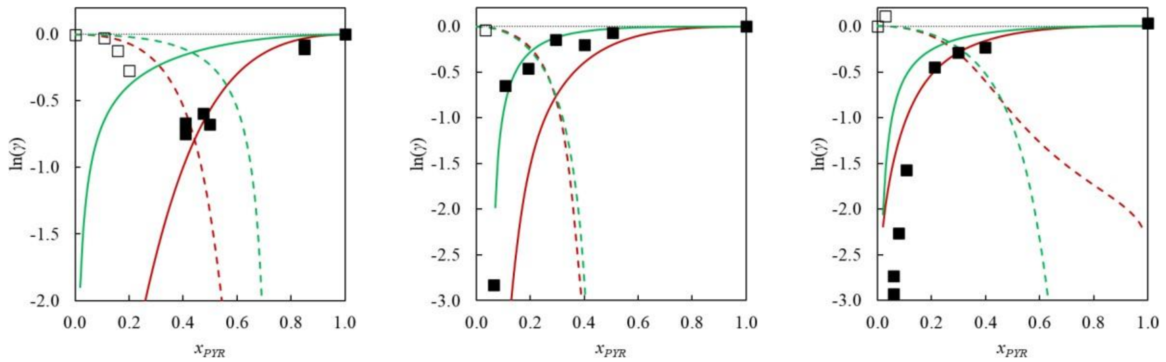

(H) (I) (J)

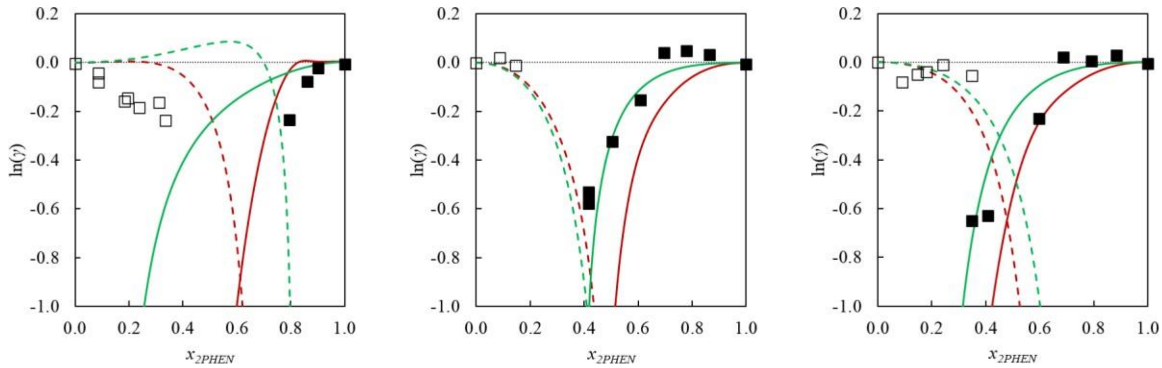

Figure S.5 – Non-isothermal activity coefficients of QN/PG (A), QN/THY (B), QN/BHA (C), PYR/PG (D), PYR/THY (E), PYR/BHA (F), 2PHEN/PG (G), 2PHEN/THY (H), 2PHEN/BHA (I). Symbols represent activity coefficients of the APIs (black square) and the excipients (white square). Lines represent the activity coefficient predictions of COSMO-RS with the TZVP parametrization (green lines) and TZVPD-FINE parametrization (red lines) of the APIs (solid lines) and excipients (dashed lines). Dotted horizontal lines represent the ideal behaviour, $\ln(\gamma_i) = 0$.

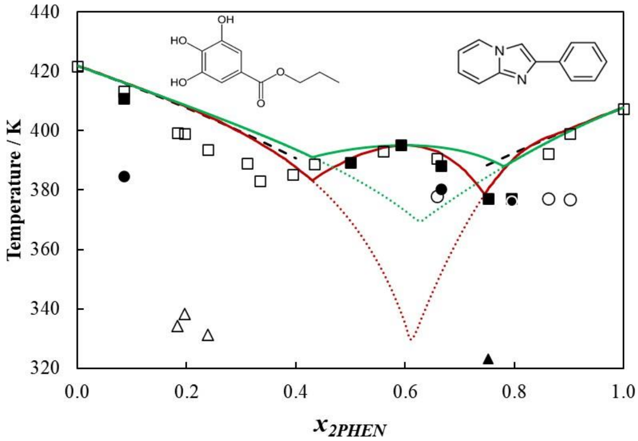

Figure S.6 – Solid-liquid phase diagrams of 2PHEN/PG. Symbols in represent melting temperatures (square), eutectic temperatures (circle) and metastable eutectic temperatures (triangle) measured using visual method (white) and using DSC (black). Lines represent the ideal model (black dashed line), COSMO-RS TZVP (green solid line), COSMO-RS TZVPD-FINE (red solid line) and metastable solubility lines using COSMO-RS TZVP (green dotted line) and COSMO-RS TZVPD-FINE (red dotted line).

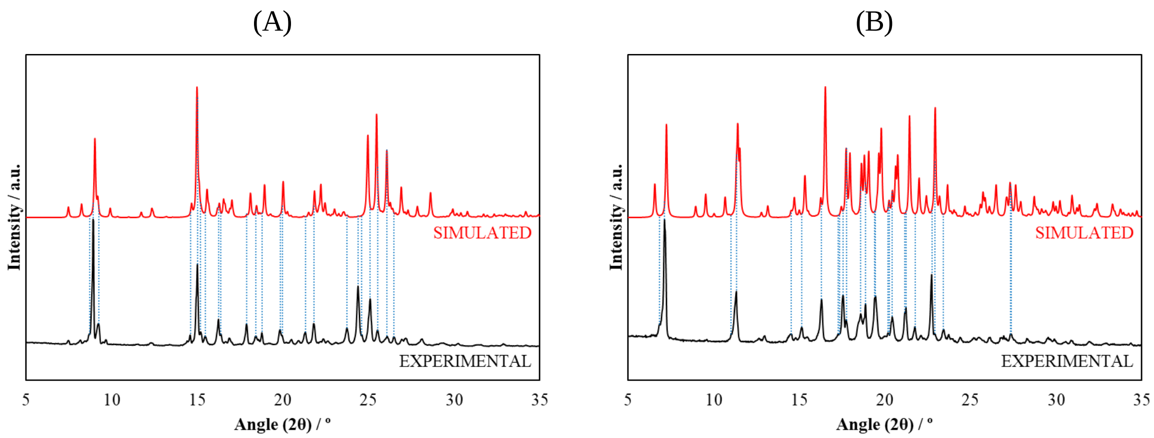

Figure S.7 – Powder X-ray diffraction patterns of the cocrystal (A) 3:2 2PHEN/PG and (B) 3:1 2PHEN/PG experimentally measured (black) and simulated by the crystal structure obtained (red). The intensities are shifted for a better comparison.

Tables

Table S.1 - Crystal data and refinement parameters

	x_{2PHEN} = 0.60	x_{2PHEN} = 0.75
Empirical Formula	$C_{59}H_{48}N_6O_{10}$	$C_{49}H_{39}N_6O_5$
M_w	1001.03	791.86
Crystal system	Triclinic	Monoclinic
Space group	$P\bar{1}$	$I2/c$
a / [Å]	10.7743(6)	26.9844(11)
b / [Å]	12.1841(6)	15.4972(10)
c / [Å]	19.8725(12)	19.8055(8)
α / [º]	81.703(2)	90
β / [º]	83.197(2)	94.648(4)
γ / [º]	77.704(2)	90
V [Å^3]	2511.8(2)	8255.1(7)
Z	2	8
D_c [Mg m^{-3}]	1.324	1.274
μ / [mm^{-1}]	0.092	0.084
F(000)	1048	3320
Crystal size [mm^3]	0.16 x 0.14 x 0.04	0.20x0.18x0.03
θ range for data collection (°)	1.943-23.179	
Index ranges	$-11\leq h\leq 11$, $-13\leq k\leq 13$, $-21\leq l\leq 21$	
Reflections collected	32046	
Unique reflections, [R_{int}]	7004[0.0649]	
Final R indices		
R_1, wR_2 [I>2σI]	0.1169, 0.3056 [4945]	
R_1, wR_2 (all data)	0.1524, 0.3398	
Data/restraints/ parameters	7004/1/667	
Goodness-of-fit on F^2	1.057	

Table S.2 - Experimental solid-liquid equilibrium data (x, T_{eut}, T_m) for the system QN/PG. The activity coefficients (γ) were obtained as per Eq. 2 using the melting properties reported in Table 1.

x_{QN}	T_m / K [a]	T_{eut} / K [a]	γ_{QN}	γ_{PG}	Solid phase *	Measuring method
0.00	421.9	-	-	-	Propyl gallate	[1]
0.098±0.005	408.7±2.0	-	-	0.92±0.03	Propyl gallate	Visual Method
0.184±0.005	404.2±1.9	373.2†	-	0.94±0.02	Propyl gallate	Visual Method
0.297±0.005	390.8±1.0	374.9±0.8	-	0.86±0.02	Propyl gallate	Visual Method
0.388±0.005	-	377.7±1.6	0.42±0.02	0.75±0.02	-	Visual Method
0.400±0.005	379.8±2.1	-	0.43±0.03	-	Quinine	Visual Method
0.429±0.006	385.9±1.8	-	0.52±0.03	-	Quinine	Visual Method
0.500±0.006	396.9±1.0	-	0.58±0.02	-	Quinine	Visual Method
0.501±0.006	397.9±1.9	378.4±1.6	0.60±0.03	-	Quinine	Visual Method
0.611±0.007	410.4±0.9	-	0.68±0.02	-	Quinine	Visual Method
0.685±0.008	420.8±0.2	-	0.78±0.01	-	Quinine	Visual Method
0.791±0.009	430.5±0.6	-	0.85±0.02	-	Quinine	Visual Method
0.90±0.01	443.8±1.1	-	1.00±0.03	-	Quinine	Visual Method
1.00	449.0±0.2	-	-	-	Quinine	DSC

[a] Mean ± standard deviation, except †single measurements. Standard uncertainties of single measurements are estimated to be 2.0 K for visual method and 1.0 K for DSC. *Crystallized solid phase at the liquidus temperature.

Table S.3 - Experimental solid-liquid equilibrium data (x, T_{eut}, T_m) for the system QN/THY. The activity coefficients (γ) were obtained as per Eq. 2 using the melting properties reported in Table 1.

x_{QN}	T_m / K [a]	T_{eut} / K [a]	γ_{QN}	γ_{THY}	**Solid phase ***	**Measuring method**
0.000	323.3	-	-	-	Thymol	[2]
0.098±0.003	315.3†	-	-	0.92±0.02	Thymol	DSC
0.105±0.003	315.0±0.5	-	-	0.92±0.01	Thymol	Visual Method
0.148±0.006	314.9†	-	-	0.97±0.02	Thymol	DSC
0.200±0.003	315.2†	309.5†	-	1.03±0.03	Thymol	DSC
0.201±0.004	314.4±1.6	-	-	1.02±0.04	Thymol	Visual Method
0.246±0.003	-	305.7†	0.050±0.002	0.87±0.02	-	DSC
0.324±0.005	340.0±1.9	-	0.15±0.01	-	Quinine	Visual Method
0.40±0.01	370.5†	-	0.34±0.01	-	Quinine	DSC
0.503±0.007	402.2±1.0	-	0.67±0.04	-	Quinine	Visual Method
0.551±0.005	409.5±0.9	-	0.73±0.02	-	Quinine	Visual Method
0.593±0.005	416.0±1.1	-	0.83±0.02	-	Quinine	Visual Method
0.593±0.005	417.7±0.7	-	0.80±0.01	-	Quinine	Visual Method
0.600±0.006	410.7†	-	0.69±0.02	-	Quinine	DSC
0.671±0.009	428.7±1.4	-	0.96±0.03	-	Quinine	Visual Method
0.787±0.008	435.8±0.8	-	0.96±0.02	-	Quinine	Visual Method
0.790±0.008	432.8†	-	0.89±0.02	-	Quinine	DSC
0.889±0.007	444.3±0.4	-	1.02±0.01	-	Quinine	Visual Method
1.000	449.0±0.2	-	-	-	Quinine	DSC

[a] Mean ± standard deviation, except †single measurements. *Crystallized solid phase at the liquidus temperature.

Table S.4 - Experimental solid-liquid equilibrium data (x, T_{eut}, T_m) for the system QN/BHA. The activity coefficients (γ) were obtained as per Eq. 2 using the melting properties reported in Table 1.

x_{QN}	T_m / K [a]	T_{eut} / K [a]	γ_{QN}	γ_{BHA}	**Solid phase ***	**Measuring method**
0.000	332.4±0.1	-	-	-	BHA	DSC
0.045±0.004	329.6±1.7	-	-	0.97±0.04	BHA	Visual Method
0.091±0.004	325.9†	319.2†	-	0.93±0.02	BHA	DSC
0.126±0.005	324.2±1.5	-	-	0.92±0.04	BHA	Visual Method
0.198±0.005	321.3±1.0	-	0.12±0.01	0.93±0.03	BHA	Visual Method
0.247±0.004	324.0†	319.6†	0.105±0.005	-	Quinine	DSC
0.252±0.006	327.3±2.4	-	0.12±0.01	-	Quinine	Visual Method
0.292±0.006	331.7±2.0	-	0.12±0.01	-	Quinine	Visual Method
0.341±0.007	356.6±2.7	321.2†	0.25±0.02	-	Quinine	Visual Method
0.400±0.007	369.3±3.4	321.2†	0.34±0.04	-	Quinine	Visual Method
0.409±0.005	363.7†	-	0.26±0.01		Quinine	DSC
0.479±0.008	392.0±1.5	319.2†	0.52±0.02	-	Quinine	Visual Method
0.60±0.01	414.6±2.4	-	0.79±0.05	-	Quinine	Visual Method
0.69±0.01	425.2±1.6	-	0.84±0.03	-	Quinine	Visual Method
0.81±0.01	433.6±1.4	-	0.87±0.03	-	Quinine	Visual Method
0.90±0.02	442.8±0.8	-	0.96±0.02	-	Quinine	Visual Method
1.000	449.0±0.2	-	-	-	Quinine	DSC

[a] Mean ± standard deviation, except †single measurements. *Crystallized solid phase at the liquidus temperature.

Table S.5 - Experimental solid-liquid equilibrium data (x, T_{eut}, T_{per}, T_m) for the system PYR/PG. The activity coefficients (γ) were obtained as per Eq. 2 using the melting properties reported in Table 1.

x_{PYR}	T_m / K [a]	T_{eut} / K [a]	T_{per} / K [a]	γ_{PYR}	γ_{PG}	**Solid phase ***	**Measuring method**
0.000	421.9	-	-	-	-	Propyl Gallate	[1]
0.11±0.03	412.8±0.6	-	-	-	0.97±0.04	Propyl Gallate	Visual Method
0.16±0.03	403.4±1.4	-	-	-	0.88±0.04	Propyl Gallate	Visual Method
0.20±0.03	391.3†	393.1†	-	-	0.76±0.03	-	Visual Method
0.22±0.03	402.3±1.4	-	-	-	-	Cocrystal 1:1	Visual Method
0.22±0.03	409.6†	393.3†	-	-	-	Cocrystal 1:1	DSC
0.26±0.03	416.8±2.6	392.7±2.1	-	-	-	Cocrystal 1:1	Visual Method
0.27±0.03	430.0±2.7	-	-	-	-	Cocrystal 1:1	Visual Method
0.27±0.03	428.2†	392.5†	-	-	-	Cocrystal 1:1	DSC
0.30±0.03	434.6†	393.5†	-	-	-	Cocrystal 1:1	DSC
0.35±0.03	443.2±3.6	393.2†	-	-	-	Cocrystal 1:1	Visual Method
0.35±0.03	438.9±1.5	-	-	-	-	Cocrystal 1:1	Visual Method
0.41±0.03	442.4±0.5	396.0±0.3	-	0.47±0.03	-	Cocrystal 1:1	Visual Method
0.41±0.03	445.5†	388.7†	-	0.51±0.04	-	Cocrystal 1:1	DSC
0.48±0.03	453.8±0.5	-	-	0.55±0.03	-	Pyrimethamine	Visual Method
0.48±0.03	-	-	446.3†	-	-	Pyrimethamine	DSC
0.498±0.007	452.5†	-	445.4†	0.51±0.02	-	Pyrimethamine	DSC
0.60±0.03	-	-	441.1†	-	-	Pyrimethamine	DSC
0.69±0.03	-	-	446.6†	-	-	Pyrimethamine	DSC
0.85±0.04	499.7±0.8	390.8†	-	0.90±0.05	-	Pyrimethamine	Visual Method
0.85±0.04	500.9†	385.7†	446.3†	0.92±0.05	-	Pyrimethamine	DSC
1.000	512.9±0.3	-	-	-	-	Pyrimethamine	DSC

[a] Mean ± standard deviation, except †single measurements. *Crystallized solid phase at the liquidus temperature.

Table S.6 - Experimental solid-liquid equilibrium data (x, T_{eut}, T_m) for the system PYR/THY. The activity coefficients (γ) were obtained as per Eq. 2 using the melting properties reported in Table 1.

x_{PYR}	T_m / K [a]	T_{eut} / K [a]	γ_{PYR}	γ_{THY}	**Solid phase ***	**Measuring method**
0.000	323.3	-	-	-	Thymol	[2]
0.03±0.02	319.9†	-	-	0.96±0.03	Thymol	DSC
0.07±0.02	333.2†	319.2†	0.06±0.02	-	Pyrimethamine	DSC
0.11±0.02	401.0†	317.8†	0.5±0.1	-	Pyrimethamine	DSC
0.19±0.01	426.0†	316.8†	0.64±0.04	-	Pyrimethamine	DSC
0.29±0.03	452.6±1.9	316.2±0.8	0.87±0.09	-	Pyrimethamine	Visual Method
0.40±0.01	462.7†	-	0.82±0.03	-	Pyrimethamine	DSC
0.50±0.03	477.9†	-	0.94±0.06	-	Pyrimethamine	DSC
1.000	512.9±0.3	-	-	-	Pyrimethamine	DSC

[a] Mean ± standard deviation, except †single measurements. *Crystallized solid phase at the liquidus temperature.

Table S.7 - Experimental solid-liquid equilibrium data (x, T_{eut}, T_m) for the system PYR/BHA. The activity coefficients (γ) were obtained as per Eq. 2 using the melting properties reported in Table 1.

x_{PYR}	T_m / K [a]	T_{eut} / K [a]	γ_{PYR}	γ_{BHA}	Solid phase *	Measuring method
0.000	332.4±0.1	-	-	-	BHA	DSC
0.03±0.03	336.0±0.1	332.4±0.5	-	1.12±0.03	BHA	Visual Method
0.06±0.03	329.3†	323.6†	0.06±0.03	-	Pyrimethamine	DSC
0.06±0.03	333.4±0.2	329.8±0.3	0.07±0.03	-	Pyrimethamine	Visual Method
0.08±0.03	349.8±0.6	325.7±0.2	0.11±0.04	-	Pyrimethamine	Visual Method
0.11±0.03	374.3±0.1	325.9±0.4	0.21±0.05	-	Pyrimethamine	Visual Method
0.21±0.03	429.6±2.8	326.4±0.1	0.6±0.1	-	Pyrimethamine	Visual Method
0.30±0.03	447.9±1.9	327.1±0.1	0.75±0.08	-	Pyrimethamine	Visual Method
0.40±0.03	461.3±2.5	-	0.80±0.07	-	Pyrimethamine	Visual Method
1.000	512.9±0.3	-	-	-	Pyrimethamine	DSC

[a] Mean ± standard deviation, except †single measurements. *Crystallized solid phase at the liquidus temperature.

Table S.8 - Experimental solid-liquid equilibrium data (x, T_{eut}, T_m) for the system 2PHEN/PG. The activity coefficients (γ) were obtained as per Eq. 2 using the melting properties reported in Table 1.

x_{2PHEN}	T_m / K [a]	T_{eut} / K [a]	γ_{2PHEN}	γ_{PG}	Solid phase *	Measuring method
0.000	421.9	-	-	-	Propyl Gallate	[1]
0.09±0.04	413.3±0.6	-	-	0.96±0.04	Propyl Gallate	Visual Method
0.09±0.04	411.0†	384.7†	-	0.92±0.04	Propyl Gallate	DSC
0.18±0.04	399.2±1.9	-	-	0.85±0.05	Propyl Gallate	Visual Method
0.20±0.03	399.1±0.5	-	-	0.86±0.04	Propyl Gallate	Visual Method
0.24±0.03	393.7±1.4	-	-	0.83±0.04	Propyl Gallate	Visual Method
0.31±0.03	389.2±0.6	-	-	0.85±0.04	Propyl Gallate	Visual Method
0.33±0.03	383.2±1.9	-	-	0.79±0.04	-	Visual Method
0.39±0.03	385.3±0.9	-	-	-	Cocrystal 3:2	Visual Method
0.43±0.02	388.7±1.2	-	-	-	Cocrystal 3:2	Visual Method
0.500±0.007	389.2†	-	-	-	Cocrystal 3:2	DSC
0.56±0.03	393.2†	-	-	-	Cocrystal 3:2	Visual Method
0.592±0.007	395.1†	-	-	-	Cocrystal 3:2	DSC
0.66±0.03	390.7±0.3	378.1†	-	-	Cocrystal 3:2	Visual Method
0.666±0.007	388.3†	380.5†	-	-	Cocrystal 3:2	DSC
0.75±0.01	377.3±0.3	-	-	-	Cocrystal 3:1	DSC
0.80±0.03	377.3†	376.1†	0.79±0.03	-	2PHEN	DSC
0.86±0.03	392.2±3.2	377.2†	0.92±0.06	-	2PHEN	Visual Method
0.90±0.03	399.0±1.1	377.0±0.1	0.98±0.04	-	2PHEN	Visual Method
1.000	407.8±0.2		-	-	2PHEN	DSC

[a] Mean ± standard deviation, except †single measurements. *Crystallized solid phase at the liquidus temperature.

Table S.9 - Experimental solid-liquid equilibrium data (x, T_{eut}, T_m) for the system 2PHEN/THY. The activity coefficients (γ) were obtained as per Eq. 2 using the melting properties reported in Table 1.

x_{2PHEN}	T_m / K [a]	T_{eut} / K [a]	γ_{2PHEN}	γ_{THY}	Solid phase *	Measuring method
0.000	323.3	-	-	-	Thymol	[2]
0.09±0.03	320.1±0.6	315.6±0.2	-	1.02±0.04	Thymol	Visual Method
0.15±0.03	315.9†	315.9†	-	0.99±0.04	-	DSC
0.22±0.03	324.8†	315.4†	-	-	Cocrystal 1:2	DSC
0.29±0.03	329.9±0.1	316.2±0.1	-	-	Cocrystal 1:2	Visual Method
0.332±0.007	329.1±0.4	-	-	-	Cocrystal 1:2	Visual Method
0.332±0.007	329.7±0.3	-	-	-	Cocrystal 1:2	DSC
0.36±0.03	329.7±0.5	317.5±1.6	-	-	Cocrystal 1:2	Visual Method
0.42±0.03	327.4±1.6	-	0.59±0.05	-	-	Visual Method
0.42±0.03	325.2†	311.0†	0.56±0.04	-	-	DSC
0.50±0.03	346.8±1.4	-	0.72±0.05	-	2PHEN	Visual Method
0.61±0.03	366.2†	328.9†	0.86±0.05	-	2PHEN	DSC
0.69±0.04	386.1±2.6	-	1.04±0.07	-	2PHEN	Visual Method
0.78±0.04	393.9†	329.8†	1.05±0.05	-	2PHEN	DSC
0.86±0.04	399.8±1.2	-	1.03±0.05	-	2PHEN	Visual Method
1.000	407.8±0.2	-	-	-	2PHEN	DSC

[a] Mean ± standard deviation, except †single measurements. *Crystallized solid phase at the liquidus temperature.

Table S.10 - Experimental solid-liquid equilibrium data (x, T_{eut}, T_m) for the system 2PHEN/BHA. The activity coefficients (γ) were obtained using Eq. 2 using the melting properties reported in Table 1.

x_{2PHEN}	T_m / K [a]	T_{eut} / K [a]	γ_{2PHEN}	γ_{BHA}	Solid phase *	Measuring method
0.000	332.4±0.1	-	-	-	BHA	DSC
0.09±0.03	325.9†	-	-	0.92±0.04	BHA	DSC
0.15±0.03	324.3±0.8	-	-	0.95±0.04	BHA	Visual Method
0.18±0.03	323.3±1.5	-	-	0.96±0.05	BHA	Visual Method
0.24±0.03	321.4±1.0	-	-	0.99±0.05	BHA	Visual Method
0.35±0.03	314.2†	311.7†	0.52±0.05		2PHEN	DSC
0.41±0.03	322.1†	316.3†	0.53±0.04	-	2PHEN	DSC
0.46±0.03	331.0†	314.7†	0.58±0.04	-	2PHEN	DSC
0.60±0.03	360.8†	314.9†	0.80±0.05	-	2PHEN	DSC
0.69±0.03	381.0±1.0	-	1.02±0.05	-	2PHEN	Visual Method
0.79±0.04	392.1±1.3	-	1.00±0.05	-	2PHEN	Visual Method
0.89±0.04	401.2†	-	1.03±0.05	-	2PHEN	Visual Method
1.000	407.8±0.2	-	-	-	2PHEN	DSC

[a] Mean ± standard deviation, except †single measurements. *Crystallized solid phase at the liquidus temperature.

Table S.11 - Activity coefficients (γ) predicted by COSMO-RS with TZVP parametrization at 298.15 K.

	$\ln(\gamma)$ at 1:1 molar ratio composition						$\ln(\gamma_{API}^{\infty})$		
	Excip.	**QN**	**Excip.**	**PYR**	**Excip.**	**2PHEN**	**QN**	**PYR**	**2PHEN**
Propyl Gallate	-0.36	-0.50	-0.44	-0.67	-0.13	-0.35	-3.18	-4.07	-1.85
Thymol	-0.50	-0.24	-0.44	-0.20	-0.29	-0.19	-5.67	-5.52	-3.56
BHA	-0.32	-0.20	-0.33	-0.22	-0.16	-0.16	-3.05	-3.54	-2.01
Vanillin	0.09	-0.03	-0.20	-0.26	0.09	0.02	-0.09	-2.42	-0.35
Acetovanillin	0.00	0.00	-0.23	-0.18	-0.02	-0.02	-0.05	-1.94	-0.39
4-Hydroxybenzaldehyde	0.00	-0.11	-0.23	-0.28	0.05	-0.05	-0.58	-2.60	-0.60
Syringaldehyde	0.02	0.01	-0.25	-0.22	-0.02	-0.02	0.08	-2.08	-0.38
Propylparaben	-0.18	-0.19	-0.28	-0.32	-0.04	-0.12	-1.56	-2.73	-0.95
Betaine	0.00	-0.07	-0.81	-0.34	-0.12	0.46	-5.45	-8.07	-2.56
ChCl	0.66	0.71	-0.19	0.18	0.24	0.75	-0.46	-4.41	-0.72
$[N_{1111}]Cl$	0.19	0.18	-0.57	-0.23	-0.02	0.38	-2.47	-6.06	-1.71
Menthol	0.09	0.05	0.14	0.12	0.27	0.24	0.72	0.56	1.64
Gallic Acid	0.60	0.00	0.15	-0.32	0.45	0.25	0.90	-2.01	0.51

Table S.12 - Activity coefficients (γ) predicted by COSMO-RS with TZVP parametrization at 423.15 K.

	$\ln(\gamma)$ at 1:1 molar ratio composition						$\ln(\gamma_{API}^{\infty})$		
	Excip.	**QN**	**Excip.**	**PYR**	**Excip.**	**2PHEN**	**QN**	**PYR**	**2PHEN**
Propyl Gallate	-0.22	-0.26	-0.28	-0.34	-0.08	-0.14	-0.90	-1.13	-0.34
Thymol	-0.26	-0.12	-0.17	-0.08	-0.11	-0.06	-1.15	-0.74	-0.42
BHA	-0.17	-0.11	-0.15	-0.10	-0.06	-0.05	-0.72	-0.59	-0.23
Vanillin	0.12	0.03	-0.09	-0.10	0.10	0.08	0.53	-0.38	0.39
Acetovanillin	-0.01	-0.01	-0.16	-0.12	-0.01	-0.01	-0.04	-0.65	-0.03
4-Hydroxybenzaldehyde	0.05	-0.02	-0.11	-0.12	0.07	0.04	0.28	-0.46	0.29
Syringaldehyde	0.01	0.01	-0.18	-0.15	-0.01	0.00	0.04	-0.71	-0.03
Propylparaben	-0.10	-0.09	-0.16	-0.16	-0.01	-0.03	-0.40	-0.62	-0.03
Betaine	0.16	0.16	-0.51	-0.12	0.00	0.44	-1.14	-3.03	-0.53
ChCl	0.68	0.65	-0.01	0.25	0.31	0.67	1.50	-0.89	0.79
$[N_{1111}]Cl$	0.27	0.24	-0.34	-0.07	0.07	0.36	-0.10	-2.11	-0.11
Menthol	0.07	0.04	0.11	0.10	0.20	0.18	0.28	0.45	0.81
Gallic Acid	0.60	0.23	0.21	0.04	0.42	0.40	2.34	0.65	1.60

Table S.13 - Melting properties of the compounds used for COSMO-RS predictions.

Compound	T_m / K	$\Delta_m H$ / kJ·mol^{-1}	Reference
Betaine	566.15	17.98	[3]
Choline Chloride	597	4.3	[4]
Tetramethyl ammonium chloride	612.9	20.5	[5]
Gallic Acid	524.2	62.4	[6]
(-)-Menthol	315.7	12.9	[7]
Acetovanillone	-	-	-
Vanillin	355.4	22.4	[8]
4-Hydroxybenzaldehyde	390.8	21.6	[8]
Syringaldehyde	385.6	31.3	[9]
Propylparaben	369.3	27.2	[10]

References

(1) Gao, Z.; Li, Z.; Li, M.; Wang, Z.; Zhou, R.; Wang, B. Solubility Measurement and Thermodynamic Model Correlation of Propyl Gallate in Pure and Binary Solvents from T = (293.15 to 333.15) K. *J Mol Liq* **2020**, *318*, 114035. https://doi.org/10.1016/j.molliq.2020.114035.

(2) Teixeira, G.; Abranches, D. O.; Silva, L. P.; Vilas-Boas, S. M.; Pinho, S. P.; Ferreira, A. I. M. C. L.; Santos, L. M. N. B. F.; Ferreira, O.; Coutinho, J. A. P. Liquefying Flavonoids with Terpenoids through Deep Eutectic Solvent Formation. *Molecules* **2022**, *27* (9), 2649. https://doi.org/10.3390/molecules27092649.

(3) Wang, S.; Zhang, Y.; Wang, J. Solubility Measurement and Modeling for Betaine in Different Pure Solvents. *J Chem Eng Data* **2014**, *59* (8), 2511–2516. https://doi.org/10.1021/je500267w.

(4) Fernandez, L.; Silva, L. P.; Martins, M. A. R.; Ferreira, O.; Ortega, J.; Pinho, S. P.; Coutinho, J. A. P. Indirect Assessment of the Fusion Properties of Choline Chloride from Solid-Liquid Equilibria Data. *Fluid Phase Equilib* **2017**, *448*, 9–14.

(5) Pontes, P. V. A.; Crespo, E. A.; Martins, A. R.; Silva, L. P.; Pontes, P. V. A.; Crespo, E. A.; Neves, C. M. S. S.; Maximo, G. J.; Dupas, M.; Pinho, P.; Coutinho, A. P.; Sadowski, G.; Batista, E. A. C.; Held, C. Measurement and PC-SAFT Modeling of Solid-Liquid Equilibrium of Deep Eutectic Solvents of Quaternary Ammonium Chlorides and Carboxylic Acids. *Fluid Phase Equilib* **2017**, *448*, 69–80.

(6) Bogel-Łukasik, R.; Nobre Gonçalves, L. M.; Bogel-Łukasik, E. Phase Equilibrium Phenomena in Solutions Involving Tannins, Flavonoids and Ionic Liquids. *Green Chemistry* **2010**, *12* (11), 1947. https://doi.org/10.1039/c0gc00308e.

(7) Martins, M. R.; Crespo, E. A.; Pontes, P. V. A.; Silva, L. P.; Bülow, M.; Maximo, G. J.; Batista, E. A. C.; Held, C.; Pinho, S. P.; Coutinho, J. A. P. Tunable Hydrophobic Eutectic Solvents Based on Terpenes and Monocarboxylic Acids. *ACS Sustainable Chemistry & Engineering* **2018**, *6* (7), 8836–8846.

(8) Temprado, M.; Roux, M. V.; Chickos, J. S. Some Thermophysical Properties of Several Solid Aldehydes. *J Therm Anal Calorim* **2008**, *94* (1), 257–262. https://doi.org/10.1007/s10973-007-8883-0.

(9) Almeida, A. R. R. P.; Pinheiro, B. D. A.; Ferreira, A. I. M. C. L.; Monte, M. J. S. Study on the Volatility of Four Benzaldehydes. *Thermochim Acta* **2022**, *717*, 179357. https://doi.org/10.1016/j.tca.2022.179357.

(10) Giordano, F.; Bettini, R.; Donini, C.; Gazzaniga, A.; Caira, M. R.; Zhang, G. G. Z.; Grant, D. J. W. Physical Properties of Parabens and Their Mixtures: Solubility in Water, Thermal Behavior, and Crystal Structures. *J Pharm Sci* **1999**, *88* (11), 1210–1216. https://doi.org/10.1021/js9900452.